JOURNAL OF BACTERIOLOGY, Feb. 1996, p. 1018–1029 Vol. 178, No. 4
0021-9193/96/$04.00+0

Membrane-Associated Methane Monooxygenase from *Methylococcus capsulatus* (Bath)†

JAMES A. ZAHN AND ALAN A. DiSPIRITO*

Department of Microbiology, Immunology and Preventive Medicine, Iowa State University, Ames, Iowa 50011

Received 25 September 1995/Accepted 30 November 1995

An active preparation of the membrane-associated methane monooxygenase (pMMO) from *Methylococcus capsulatus* Bath was isolated by ion-exchange and hydrophobic interaction chromatography using dodecyl β-D-maltoside as the detergent. The active preparation consisted of three major polypeptides with molecular masses of 47,000, 27,000, and 25,000 Da. Two of the three polypeptides (those with molecular masses of 47,000 and 27,000 Da) were identified as the polypeptides induced when cells expressing the soluble MMO are switched to culture medium in which the pMMO is expressed. The 27,000-Da polypeptide was identified as the acetylene-binding protein. The active enzyme complex contained 2.5 iron atoms and 14.5 copper atoms per 99,000 Da. The electron paramagnetic resonance spectrum of the enzyme showed evidence for a type 2 copper center ($g_\perp = 2.057$, $g_\parallel = 2.24$, and $|A_\parallel| = 172$ G), a weak high-spin iron signal ($g = 6.0$), and a broad low-field ($g = 12.5$) signal. Treatment of the pMMO with nitric oxide produced the ferrous-nitric oxide derivative observed in the membrane fraction of cells expressing the pMMO. When duroquinol was used as a reductant, the specific activity of the purified enzyme was 11.1 nmol of propylene oxidized · min^{-1} · mg of $protein^{-1}$, which accounted for approximately 30% of the cell-free propylene oxidation activity. The activity was stimulated by ferric and cupric metal ions in addition to the cytochrome *b*-specific inhibitors myxothiazol and 2-heptyl-4-hydroxyquinoline-*N*-oxide.

In methanotrophs, the oxidation of methane to methanol is catalyzed by the methane monooxygenase (MMO) (31). In some genera, either a soluble or a membrane-associated MMO is present depending on the copper concentration during growth (13, 43, 50, 54). At low copper-to-biomass ratios, the enzyme activity occurs in the soluble fraction and is referred to as the soluble MMO (sMMO). At higher copper-to-biomass ratios, methane oxidation activity is catalyzed in the membrane fraction by the membrane-associated or particulate MMO (pMMO). The polypeptides and genes for the sMMO in several different methanotrophs have been characterized (10, 18, 19, 22–24, 34, 41, 42, 54). The pMMO has proven more elusive. There is indirect evidence that the enzyme contains copper, and inhibitor studies indicate that the enzyme is coupled to the electron transport chain (13, 40, 52, 54). In addition, three polypeptides with molecular masses of 46,000, 35,000, and 26,000 Da are induced when cells expressing the sMMO convert to expression of pMMO under altered growth conditions (13, 54). Tonge et al. (55) reported the solubilization of methane-oxidizing activity from *Methylosinus trichosporium* OB3b with phospholipase C or by sonification. A three-subunit enzyme with subunit molecular masses of 47,000, 13,000, and 9,400 Da was isolated from this solubilized fraction. The 13,000-Da polypeptide was a CO-binding *c*-type cytochrome. The 47,000-Da polypeptide contained approximately one copper atom per molecule, and the 9,400-Da polypeptide was reported to be a regulatory protein. The purified enzyme could use ascorbate but not NADH as a reductant. Akent'eva and Govozdev (1) also reported the isolation of a membrane-associated, methane-oxidizing enzyme which utilized NADH as a reductant from *Methylococcus capsulatus*. This enzyme was composed of two subunits, with molecular masses 45,000 and 35,000 Da, in an $\alpha_4\beta_4$ subunit structure, with 4 mol of nonheme iron and 1 mol of copper per mol of enzyme complex. However, attempts to reproduce these results in this and other laboratories have not been successful.

The present report describes a reproducible procedure for the solubilization and isolation of the pMMO from *M. capsulatus* Bath. The paper focuses initially on the optimization of culture conditions for the isolation of this enzyme and then on the isolation and initial characterization of the pMMO. Four observations aided in the stabilization and isolation of the pMMO from *M. capsulatus* Bath. First, increased copper and iron concentrations in the culture medium resulted in increased pMMO activity in the washed membrane fraction. Second, the pMMO contains at least one iron atom center. Third, the addition of high concentrations of iron as well as copper to the growth medium were required for optimal cell-free pMMO activity. Fourth, maintaining anaerobic conditions during solubilization from the membrane fraction stabilized cell-free pMMO activity.

MATERIALS AND METHODS

Organism and cultivation. *M. capsulatus* Bath was grown in nitrate mineral salts (NMS) media (57) plus 0, 0.2, 0.5, 1.0, 2.5, 5.0, 10.0, or 20.0 μM $CuSO_4$ and a vitamin mixture (30) at 37°C under an atmosphere of 40% methane, 20% oxygen, and 40% air (vol/vol/vol). Cells grown under low (i.e., no copper addition)-copper conditions were cultured by a semicontinuous method using NMS medium plus a vitamin mixture under copper limitation at 37°C in a 12-liter fermentor sparged at flow rates between 80 and 150 ml of methane per min and 2,000 to 2,500 ml of air per min. Cell batches exhibiting less than 100% sMMO activity (typically the first and second batches) were discarded.

Cells cultured for the isolation of the pMMO were grown in NMS medium plus 5 μM $CuSO_4$. The copper concentration in the growth medium was increased as the cell density increased. When the cells reached an optical density at 600 nm of 0.3 to 0.4, the copper and iron concentrations were increased incrementally by the addition of 10 μM $CuSO_4$, 5 μM ferric EDTA, and 5 μM

* Corresponding author. Mailing address: Department of Microbiology, Immunology and Preventive Medicine, Iowa State University, 205 Science Building I, Ames, IA 50011-3211. Phone: (515) 294-2944. Fax: (515) 294-6019. Electronic mail address: aland@iastate.edu.

† This journal paper, J-16372, is a contribution from the Agriculture and Home Economics Experiment Station, Ames, Iowa (project 3252).

ferrous sulfate every 6 to 8 h to final concentrations of 60 μM copper and 60 μM iron at late log phase (optical density at 600 nm = 1.4 to 1.7). Cells were harvested by centrifugation at 13,000 × *g* for 15 min at 4°C and resuspended (1:5 [wt/vol]) in 30 mM 3-[*N*-morpholino]propanesulfonic acid (MOPS), pH 7.3 (buffer A).

Isolation of washed bacterial membranes. All purification procedures were performed at 4°C under anaerobic conditions unless otherwise stated. Cells were lysed in a French pressure cell at 18,000 lb/in^2. The homogenate was centrifuged at 12,000 × *g* for 20 min to remove unlysed cells and debris. The supernatant was then centrifuged at 140,000 × *g* for 2 h to sediment membranes. The supernatant was discarded, and the membranes were resuspended by using a Dounce homogenizer in buffer A containing 1 M KCl and centrifuged for 2 h at 140,000 × *g*. The supernatant was discarded, and the salt-washed membrane pellet was resuspended in 50 ml of buffer A by using a Dounce homogenizer and stored under deoxygenated argon.

Isolation of the pMMO. The membrane suspension was transferred into a 125-ml serum vial sealed with a Teflon-silicone septum and deoxygenated for several cycles of vacuum followed by reduced (i.e., deoxygenated through a heated copper column) argon. The anaerobic membrane fraction was transferred into an anaerobic chamber at room temperature, and the solution was stirred for 15 min under an atmosphere of 5% hydrogen and 95% nitrogen. Following equilibration of the sample, a 10% (wt/vol) solution of dodecyl β-D-maltoside was added to a final concentration of 1.4 mg of detergent per mg of protein with stirring. The solution was stirred for 45 min at room temperature and then centrifuged at 140,000 × *g* for 2 h at 4°C. The detergent-solubilized membrane fraction was diluted to a detergent/solvent ratio of 6 mg of dodecyl β-D-maltoside per ml of deoxygenated buffer A and loaded onto a DEAE-cellulose (2.5 by 28 cm) column fitted with flow adapters and equilibrated with deoxygenated buffer A. The pMMO did not bind to the column, and it eluted in the flowthrough fractions when deoxygenated buffer A was used. The flowthrough fractions were combined and loaded on a Phenyl-Sepharose column (2.5 by 24 cm) equilibrated with deoxygenated buffer A. The column was washed at a flow rate of 4 cm/h with 1 column volume of buffer A plus 0.01% dodecyl β-D-maltoside (buffer B). The pMMO fraction remained bound to the column and appeared as a diffuse, light gray band which migrated slowly through the column during the washing step with buffer B. The pMMO fraction was eluted from the column with 300 ml of a buffer containing 30 mM MOPS (pH 7.3) and 0.9% dodecyl maltoside (buffer C). The sample was concentrated under deoxygenated nitrogen at 4°C on a stirred cell (PM-30 filter) to a final protein concentration of 85.5 mg/ml. The preparations of isolated pMMO could be stored for more than 1 week under reduced argon or nitrogen at 0 to 4°C with no appreciable loss of enzyme activity.

Labeling of the pMMO with [U-^{14}C]acetylene. [U-^{14}C]acetylene was synthesized from $Ba^{14}CO_3$ (specific activity of 50 mCi/mmol) (Amersham Corp., Arlington Heights, Ill.) and barium metal as described by Hyman and Arp (27). Exactly 200 μl of isolated enzyme (12.1 mg of protein) was transferred to a 6-ml serum vial. Reduced duroquinone or ascorbate-phenazine methosulfate (PMS) were added to the vial to final concentrations of 35 μM or 10 mg/ml and 6 μM, respectively. The vial was sealed with a Teflon-silicone septum, and 12 μl of [U-^{14}C]acetylene (9.0×10^5 dpm/μl) and 1 ml of oxygen were added to the vial with a syringe. The vials were incubated on a reciprocal shaker (200 rpm) at 37°C for 1 h. Propylene oxidation activity was not detected following this treatment. The reaction was terminated by freezing the samples at −20°C for 1 h.

Whole-cell samples of *M. capsulatus* Bath were labeled with [U-^{14}C]acetylene as described by DiSpirito et al. (15). A 2-ml suspension of cells (0.1 g [wet weight] per ml of buffer A) was placed in a 6-ml vial with 2.5 mM formate. The vial was sealed, and 40 μl of [U-^{14}C]acetylene (9.0×10^5 dpm/μl) and 1 ml of oxygen were added through the septum with a syringe. Labeled cells were lysed in a French pressure cell at 18,000 lb/in^2. The homogenate was centrifuged at 12,000 × *g* for 20 min to remove unlysed cells and debris. Purified pMMO, cell free, or washed membrane polypeptides of *M. capsulatus* Bath were separated by sodium dodecyl sulfate (SDS)-polyacrylamide gel electrophoresis, and the dried gels were incubated in a phosphor storage cassette for 3 to 4 days and analyzed on a Molecular Dynamics model 400A PhosphorImager for [U-^{14}C]acetylene-labeled polypeptides.

Isolation of the 47,000- to 27,000-Da switchover polypeptides. The term "47,000- to 27,000-Da switchover polypeptides" is used to describe the polypeptides induced when cells expressing the sMMO convert to expression of pMMO under altered growth conditions (54). The salt-washed membrane pellet was resuspended in 10 mM Tris-HCl, pH 8.0 (buffer D), plus 1.5% (wt/vol) Triton X-100 (Surfact Amps; Perice Chemical Co., Rockford, Ill.) to a final protein concentration of 16 mg/ml with a Dounce homogenizer. The suspension was incubated for 1 h with stirring and centrifuged at 140,000 × *g* for 2 h. The supernatant was dialyzed against six changes of buffer D plus 0.01% Triton X-100 (buffer E) and loaded on a DEAE-cellulose column (2.5 by 15 cm) equilibrated with buffer E. The flowthrough fractions were collected and loaded on a DEAE-Sepharose CL-6B column (2.5 by 28 cm) equilibrated with buffer E. The column was developed with a linear gradient of 0 to 1 M KCl in buffer D followed by a linear gradient of 0.01 to 1.4% Triton X-100 plus 1 M KCl in buffer D. Fractions which eluted at approximately 0.8% (wt/vol) Triton X-100 were collected and dialyzed against three changes of buffer D. Following dialysis, the sample was loaded on a DEAE-Sepharose CL-6B column (1.25 by 10 cm) equilibrated with buffer D. The column was washed with 200 ml of 1 mM 3-[(3-cholamidopropyl)-dimethyl-ammonio]-1-propanesulfonate (CHAPS) in buffer D and eluted with buffer D plus 1% CHAPS, 1% octyl-glycoside, and 1 M KCl. The samples were dialyzed against three changes of buffer B plus 1 mM CHAPS and concentrated with a stirred cell (PM-30 filter). The sample was loaded onto a 5 to 20% sucrose density gradient containing 500 mM potassium phosphate (pH 7.0) with 2 mM CHAPS and centrifuged for 12 h at 130,000 × *g*. The major, gray or tan band at the bottom of the tube (47,000- to 27,000-Da switchover polypeptides) and a brown-red band at the top of the tube (cytochrome *b*-559/569) were collected and dialyzed for 12 h against three changes of buffer D plus 1 mM CHAPS.

Isolation of the copper-binding cofactor (cbc) from washed membranes. Salt-washed membranes were resuspended in 5 mM CHAPS with a Dounce homogenizer (final concentration of 30 mg of protein per ml). The solution was centrifuged at 140,000 × *g* for 2 h, and the supernatant was discarded. The pellet was resuspended in 20 to 30 times the pellet volume of 50% *N*,*N*-dimethyl formamide and centrifuged at 13,000 × *g* for 25 min. The supernatant was saved, and the pellet was resuspended in 20 to 30 times the pellet volume of 100% *N*,*N*-dimethyl formamide and centrifuged at 13,000 × *g* for 25 min. The supernatant was combined with the 50% *N*,*N*-dimethyl formamide fraction and dried under vacuum on a rotary evaporator at 60°C. The sample was resuspended in a minimal volume of 50 mM phosphate buffer, pH 7.0, and loaded on a silica gel (40 to 140 mesh) column (2.5 by 20 cm). The column was washed with 1 column volume of H_2O and 1 column volume of 50% methanol and eluted with 50% methanol plus 20 mM HCl. The sample was freeze-dried and resuspended in buffer A.

Isolation of the cbc from spent media. The cbc could also be isolated from spent media. Samples (2 g) of lyophilized spent media were resuspended in ethanol-water (65:45) solution and acidified to pH 3.6 with HCl. The solution was centrifuged at 13,000 × *g* for 10 min to remove precipitated protein. The supernatant was concentrated to approximately 5 ml by rotary evaporation at 55°C. The concentrated sample was then loaded on a Kwik desalting column (1 by 10 cm; Pierce Chemical Co., Rockford, Ill.), lyophilized, and resuspended in buffer A.

Protein, metal, and heme determinations. The concentrations of heme *a*, heme *b*, and heme *c* were measured by the pyridine hemochromogen method (14) using the Δε at 587 nm $\Delta\varepsilon_{587}$ of 21.7 cm^{-1} mM^{-1} for heme *a* (58), the $\Delta\varepsilon_{557}$ of 34.4 cm^{-1} mM^{-1} for heme *b* (58), and the $\Delta\varepsilon_{550}$ of 29.1 cm^{-1} mM^{-1} for heme *c* (20). The simultaneous determination of heme *a*, heme *b*, and heme *c* concentrations in washed membrane fractions was also performed by the method of Berry and Trumpower (7).

The separation of extractable hemes was performed by reverse-phase high-performance liquid chromatography (HPLC). Salt-washed membrane fractions (43.4 mg of protein) were extracted twice with an acetone-HCl (99:1 [vol/vol]) solution at −20°C. The combined extracts were partitioned into diethyl ether, washed twice with H_2O, and dried in a stream of nitrogen. The hemes were solubilized with 2 ml of an acetonitrile-water-trifluoroacetic acid (50:49.92:0.08) solution and filtered through a 0.45-μm-pore-size filter. The filtered heme-containing solutions were separated by gradient reverse-phase HPLC using a VyDac semipreparative C_{18} column (10 by 250 mm) at a flow rate of 4.0 ml/min with water-trifluoroacetic acid (99.9:0.1) (buffer F) and acetonitrile-trifluoroacetic acid (99.92:0.08) (buffer G) as the mobile phase. The linear gradient proceeded from 40% buffer G at 10 min following injection to 100% buffer G at 40 min. Heme standards were composed of bovine hemoglobin (protoheme) and *M. capsulatus* (Bath) cytochrome aa_3 (16). Fractions exhibiting an A_{400} were collected and lyophilized to dryness for analysis of molecular mass by matrix-assisted laser desorption ionization time-of-flight mass spectroscopy on a Finnigan LASERMAT 2000 mass spectrometer using synapinic acid as a matrix (4).

The inorganic sulfide content of samples was determined by the method of Beinert (5). Solutions of sodium sulfide were used as reference standards.

For metal analysis, samples were dialyzed for 18 h against five changes of 5 mM PIPES [piperazine-*N*,*N*′-bis(2-ethanesulfonic acid)]–5 mM Na EDTA (pH 7.0) buffer. Following dialysis, samples were diluted (50:50 [vol/vol]) in concentrated nitric acid and digested for 24 h at 110°C. After cooling, samples were brought to a volume of 25 ml with H_2O and were analyzed for sulfur, copper, iron, molybdenum, manganese, and zinc by inductively coupled plasma atomic emission spectroscopy with a model 3410 inductively coupled plasma atomic emissions spectrophotometer (Applied Research Laboratories).

Protein was assayed by the method of Lowry et al. (33) using bovine serum albumin as a standard.

Enzyme activity. MMO activity was determined by the epoxidation of propylene as previously described (15). The reductants used were duroquinol (35 mM) for pMMO-containing extracts, NADH (7 mM) for sMMO-containing extracts, and formate (2.5 mM) for whole-cell samples. The reaction was initiated by the injection of propylene (2 ml) or methane (10 to 1,000 μl) and oxygen (1 ml) through the septum of a sealed vial. Reaction mixtures were incubated at 37°C on a rotary shaker at 250 rpm.

Trichloroethylene oxidation was monitored as described by DiSpirito et al. (15).

sMMO activity was monitored by the epoxidation of propylene in the soluble fraction and by the formation of napthol from naphthalene by the method of Brusseau et al. (9).

The method for reduction of duroquinone to duroquinol was performed by a modification of the method described by Shiemke et al. (53) except that the

quinol was added as a solid and was present at higher concentrations (25 to 35 mM). Duroquinone (Sigma Chemical, St. Louis, Mo.) (0.2 g) was dissolved in approximately 20 ml of HCl-acidified (3 mM HCl in solvent) ethanol. Sodium hydrosulfite (0.28 g) was added to the solution with continuous stirring. After 3 min, sodium borohydride (0.07 g) was added, and the solution became colorless within 1 min. Stirring was discontinued, and the solution was allowed to stand for 15 min to promote full reduction of the quinone. After 15 min, the solution was diluted with 150 ml of distilled H_2O and suction filtered through Whatman no. 1 filter paper. The water-insoluble quinol remained colorless and did not pass through the filter. Finally, the quinol was washed with approximately 200 ml of H_2O to remove excess sodium hydrosulfite and sodium borohydride and dried by suction filtration. The quinol was placed in empty serum vials and stored at −20°C for no longer than 2 days before use.

The absence of sMMO activity was confirmed by a lack of methane oxidation activity in the soluble fraction, by monitoring for the formation of napthol from naphthalene (9), and by the SDS-polyacrylamide gel profile of polypeptides.

In inhibitor studies, the enzyme was preincubated for 5 min at 37°C with the inhibitor before the reaction was started by the addition of propylene. Stock solutions of 2-heptyl-4-hydroxyquinoline-*N*-oxide (HOQNO) were prepared in dimethyl sulfoxide. At the concentrations used (1 μl/ml), dimethyl sulfoxide showed no effect on the rate of propylene oxidation by the purified enzyme. Myxothiazol stock solutions were prepared in ethanol and added to empty reaction vials, and the ethanol was evaporated under a stream of reduced nitrogen. Reaction mixtures consisted of the enzyme, 35 mM duroquinol, and inhibitor in a 7-ml serum vial. Protein concentrations were 1.0 mg/ml in whole-cell assays and 3 mg/ml in pMMO assays. The reactions were initiated by injection of propylene (2 ml) and oxygen (1 ml). Reaction mixtures were incubated at 37°C on a rotary shaker at 250 rpm.

Cytochrome oxidase activity was assayed by recording oxygen uptake at 37°C in the presence of ascorbate–tetramethyl-*p*-phenylenediamine dihydrochloride as described by Ferguson-Miller et al. (17). The oxygen electrode was calibrated as previously described (46).

Spectroscopy. Optical absorption spectroscopy and X-band electron paramagnetic resonance (EPR) spectra were obtained as previously described (60). Operating parameters are outlined in the figure legends.

Anaerobic reduction and formation of nitrosyl derivatives of the washed membrane fraction. Anaerobic reduction of samples was performed in a Coy anaerobic chamber at 20°C in an atmosphere of 5% hydrogen and 95% nitrogen. Oxygen concentrations were maintained at levels below 1 ppm during all anaerobic procedures. Samples were deoxygenated on a vacuum line with repeated cycling with argon and vacuum and then transferred into the anaerobic chamber and stirred for 30 min in 3-ml reaction vials (Pierce) which were fitted with magnetic stirring bars. Following displacement of the oxygen, samples were reduced by the addition of sodium ascorbate to a final concentration of 10 mg/ml and PMS to a final concentration of 6 μM and incubated with stirring for 45 min (11). For ascorbate-PMS-reduced EPR spectra, samples were transferred from the vial to quartz EPR tubes. The tubes were capped within the anaerobic chamber and immediately frozen under liquid nitrogen following transfer from the chamber.

The nitric oxide derivatives of ascorbate-PMS-reduced samples were prepared by using the in situ reduction of the nitrite ion as the source of the nitric oxide (11). The protein-NO complex was formed anaerobically with reduced samples by adding solid $H^{14}NO_2$ or $H^{15}NO_2$ (ICL, Andover, Mass.) to a final concentration of 5 mg/ml. The samples were incubated with stirring for 30 to 60 s following the addition of nitrite and then transferred into quartz EPR tubes. The tubes were capped within the anaerobic chamber and immediately frozen under liquid nitrogen.

Preparation of antibodies against the pMMO and cytochrome *caa*$_3$–cytochrome *c*-557 complex. Cytochrome *caa*$_3$–cytochrome *c*-557 complex and the pMMO were purified as described by DiSpirito et al. (16) and as described above, respectively. Antisera against these polypeptides were raised in two 10-week-old female New Zealand White rabbits. Each enzyme (0.6 mg per rabbit) was diluted in Ribi adjuvant according to the manufacturer's recommendations and injected intradermally. Immunoglobulin G was purified from serum by using immobilized protein A (Pierce) and concentrated with a Centriprep 30 concentrator (Amicon, Inc., Beverly, Mass.).

Electrophoresis and immunoblot analysis. SDS-polyacrylamide slab gel electrophoresis was carried out by the method of Laemmli (29) on 12 to 15% gels. Unless otherwise indicated, reductants were not added to the buffers and the samples were incubated at room temperature for 10 to 30 min prior to loading. Gels were stained with Coomassie brilliant blue R for total protein or by the diaminobenzidine method (37) for *c*-type cytochromes or were blotted for immunoassays. Densitometry was performed on dried gels stained with Coomassie R-250 by using a Bioimaging Technologies Biovideo MP1000 gel documentation system.

Proteins were blotted onto nitrocellulose by using a Mini Trans-Blot electrophoretic transfer cell (Bio-Rad Laboratories, Richmond, Calif.) according to the manufacturer's directions. Following treatment with serum raised against purified protein, filter-bound antibodies were detected by the alkaline phosphatase assay according to the manufacturer's directions (Bio-Rad Laboratories).

Amino acid analysis and sequence. Amino acid analyses were performed with an Applied Biosystems 420A Derivitizer coupled to an Applied Biosystems 130A separation system. Samples were hydrolyzed under vacuum in 6 M HCl plus 1.5% phenol at 150°C for 1 h. Quantitation of cysteine was performed by conversion of cysteine residues to pyridylethyl cysteine by reaction of free protein sulfhydryls with 4-vinyl pyridine (35).

Amino acid sequence analyses were performed by Edman degradation with an Applied Biosystems 477A protein sequencer coupled to a 120A analyzer. Sequence analyses of the 47,000-, 27,000-, and 25,000-Da pMMO polypeptides were performed on overloaded samples electroblotted to polyvinylidene difluoride membranes by using a transfer buffer composed of 10 mM 3-(cyclohexylamino)-1-propanesulfonic acid (pH 11) and 10% methanol.

Mass spectrometry. The molecular mass of the cbc was determined by time-of flight mass spectrometry on a Lasermat 2000 matrix-assisted laser desorption ionization mass spectrometer (Finnigan Corporation, San Jose, Calif.). Samples of the cbc were cocrystallized with the UV-absorbing matrix, super dihydroxyl benzoic acid. The super dihydroxyl benzoic acid matrix consisted of 9 parts 2,5-dihydroxy benzoic acid and 1 part 2-hydroxy-5-methoxybenzoic acid solubilized in a solution of 70% acetonitrile, 0.1% trifluoroacetic acid, and 29.9% H_2O. An excess of analyte (15 to 30 μg/μl) was mixed with the matrix solution in a one-to-one ratio and dried on a laser target grid before the target grid was placed into the vacuum chamber.

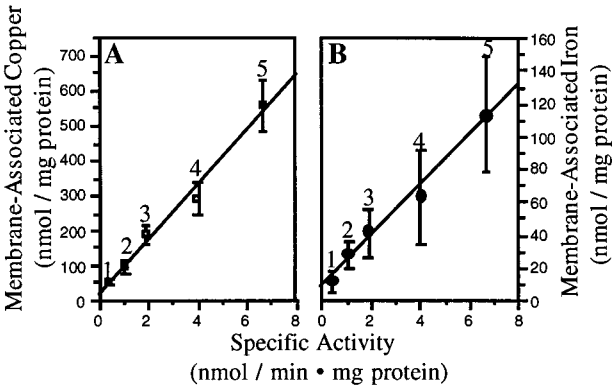

FIG. 1. Effects of copper ion concentration in the culture media on membrane-associated copper and propylene oxidation activity (A) and on membrane-associated iron and propylene oxidation activity (B). Points represent cells grown in media containing 1.0 (point 1), 2.5 (point 2), 5.0 (point 3), 10.0 (point 4), and 20.0 (point 5) μM $CuSO_4$.

RESULTS

Optimization of membrane-associated methane oxidation activity. For *M. capsulatus* Bath, pMMO activity in the washed membrane and detergent-solubilized fractions was dependent on the concentrations of copper and iron in the culture media. Consistent with previous studies (40), the concentration of copper in the growth medium stabilized methane oxidation activity in the membrane fraction (Fig. 1A). Whole-cell propylene oxidation rates for cells cultured in copper concentrations ranging from 0.5 to 20 μM remained essentially constant (85 to 125 nmol · min^{-1} · mg of $protein^{-1}$). However, the activity in the washed membrane fraction increased proportionally with the copper concentration in the growth medium.

For *M. capsulatus* Bath, copper toxicity limited the initial copper concentration of the culture media. With a 10% inoculum (optical density at 600 nm of 1 to 1.5) copper concentrations above 10 μM were toxic, and no growth was observed at initial copper concentrations greater than 20 μM. However, the copper concentration in the growth medium could be increased to greater than 20 μM when copper was added as the cell density increased (see Materials and Methods). Although the rate of whole-cell propylene oxidation activity in cells in media containing a final concentration of 60 μM $CuSO_4$ was lower (55 to 70 nmol · min^{-1} · mg of $protein^{-1}$) than the rate observed for cells cultured in 20 μM copper, the rate of activity in the detergent-solubilized fraction was 1.5- to 2.0-fold higher. Propylene oxidation activity in the 10% dodecyl β-D-maltoside

TABLE 1. Heme composition in *M. capsulatus* Bath expressing the pMMO or the sMMO[a]

Metal or heme	Concn (nmol/mg of protein) in cells expressing:				pMMO vs sMMO[b]	
	sMMO		pMMO			
	Soluble fraction	Membrane fraction	Soluble fraction	Membrane fraction	Increase	Decrease
Copper	0.7	17	0.4	189	1,012	
Iron	2.4	3.1	1.8	42	1,255	
Heme A	0	0.07	0	0.09	29	
Heme B	0	0.39	0	0.36		7.7
Heme C	1.63	0.38	1.12	0.35		8.9
Total heme	1.63	0.84	1.12	0.8		
Percent heme[c]	68	26	62	1.9		

[a] Cells expressing the pMMO were grown in NMS media supplemented with 5 μM copper sulfate.
[b] Percent difference between the metal or heme content in the membrane fractions of cells expressing the membrane-associated MMO and that in the membrane fractions of cells expressing the sMMO.
[c] Percentage of total iron in the heme fraction.

detergent extract was also stimulated 1.5-fold with the addition of equimolar concentrations of iron and copper to the culture media.

Copper-induced iron uptake. Figure 1A shows the relationship between the copper concentration in the culture media, the propylene oxidation activity, and the copper concentration in the washed membrane fraction. The results, which are similar to those obtained by Nguyen et al. (40), show an increase in both the copper concentration and the propylene oxidation rates in the membrane fraction with increased copper in the culture medium. However, in contrast to the study by Nguyen et al. (40) the results from this study showed a proportional increase in iron uptake by the membrane fraction with increased copper in the growth medium (Fig. 1B). The increased iron uptake in the washed membrane fraction from cells cultured in 0.5 to 20 μM Cu^{2+} occurred in culture media containing a constant (0.9 μM) iron concentration. The stoichiometry of iron to copper in the washed membrane fraction was 3.5 to 4.9 copper atoms per iron atom for cells expressing the pMMO. Because the increased iron uptake in the washed membrane fraction occurred in the absence of additional iron in the culture media, we refer to this phenomenon as copper-induced iron uptake. Individual datum points shown in Fig. 1 were the calculated means for 14 separate experiments.

Localization of copper-induced iron uptake. To identify the polypeptide(s) responsible for iron uptake, the total soluble and membrane-associated hemes, the extractable hemes, the concentrations of the major membrane-associated respiratory polypeptides, and the spectral properties (absorption and EPR spectroscopy) of the soluble and membrane fractions from cells expressing the pMMO were compared with those of the fractions from cells expressing the sMMO. As determined by the pyridine ferrohemochromogen assay (14), there was a difference of approximately 45% in the concentrations of heme C in the soluble fractions and a difference of less than 5% in total heme A, heme B, or heme C concentrations in the membrane fractions of cells expressing the different MMOs (Table 1).

Heme extraction, HPLC purification, and characterization by mass spectrometry were found to be efficient means by which to remove spectral interferences of cytochrome *c* in the analysis of membrane samples. The elution profiles for the extracted heme were compared with standards composed of protoheme extracted from bovine hemoglobin and *M. capsulatus* (Bath) cytochrome aa_3. Peaks eluting at 20.9 min have been assigned to protoheme because of similarities in elution profile and molecular mass of extracted protoheme from bovine hemoglobin. Comparisons of the mass spectra of the collected peaks eluting at 20.9 min showed that both samples had a molecular mass of 620 Da. This molecular mass is in good agreement with the molecular mass of protoheme, 617 Da. Peaks that elute at 29.6 min have been assigned to heme A on the basis of the elution time of heme A extracted from *M. capsulatus* (Bath) cytochrome aa_3, their molecular mass (856 Da), and the ferrohemochromogen spectral similarities to heme A extracted from *M. capsulatus* (Bath) cytochrome aa_3. Concentrations of hemes *a* and *b* in membrane fractions of cells expressing sMMO and pMMO were similar (Table 1).

Nguyen et al. (40) suggested that the increased iron in the membrane fraction was associated with cytochrome *c*-557. To determine if this cytochrome was the source of the copper-induced iron uptake, immunoblot analyses of membrane fractions isolated from cells expressing the sMMO and from cells expressing the pMMO with antibodies against cytochrome aa_3–cytochrome *c*-557 were performed. The results demonstrated that the expression levels of the polypeptides of cytochrome aa_3 and cytochrome *c*-557 were unchanged with respect to copper availability in the growth medium (data not shown). Ascorbate-tetramethyl-*p*-phenylenediamine dihydrochloride oxidase activities per milligram of protein in the membrane fractions of cells expressing the sMMO and in the membrane fractions of cells expressing the pMMO were similar.

Identification of copper-induced iron uptake: assignment of the iron environment. The EPR spectra for membrane samples show a minor increase in signals for cytochrome bb_3 ($g = 4.05$ and $g = 4.61$) from the membranes of cells expressing the sMMO. An increase in the level of type 2 copper associated with the pMMO (40) and a $g = 6.00$ signal were observed for the membranes expressing the pMMO (results not shown). Quantitation of the iron concentration by EPR integration of the $g = 6.0$ signal showed that this signal accounted for less than 15% of the increased iron associated with the membrane fraction of cells expressing the membrane-associated MMO.

Nitric oxide has been commonly used to form EPR-active nitrosyl-iron complexes in some spectroscopically indistinguishable non-heme iron enzymes (3, 39). Exposure of non-heme ferrous iron to nitric oxide can yield a species with an electronic spin of $S = 3/2$. The nitric oxide derivative EPR spectrum of the membrane fraction from cells expressing the pMMO was used to identify the source of the additional iron in the membrane fraction from cells expressing the pMMO

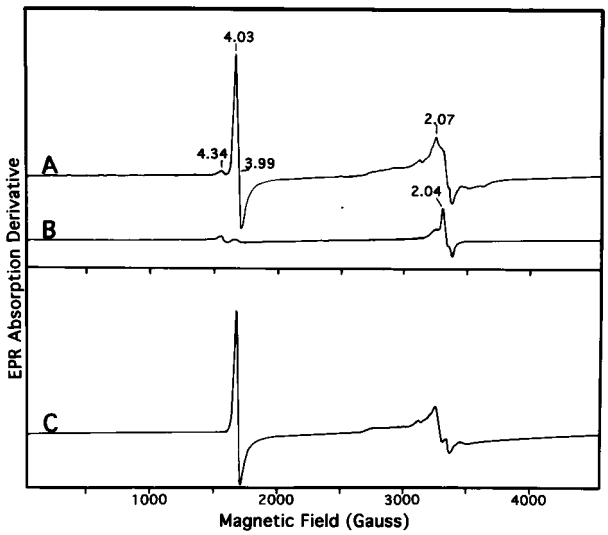

FIG. 2. EPR spectra for NO-treated, KCl-washed cell membrane fractions of *M. capsulatus* (Bath) expressing the pMMO (trace A) and the sMMO (trace B). Trace C represents spectrum A minus spectrum B. The protein concentration was 55 mg/ml in 10 mM Tris, pH 8.0, at 7.7 K. Operating parameters were as follows: modulation frequency, 100 kHz; modulation amplitude, 12.5 G; and time constant, 100 ms. The microwave frequency was 9.421 GHz, and the microwave power was 2.2 mW.

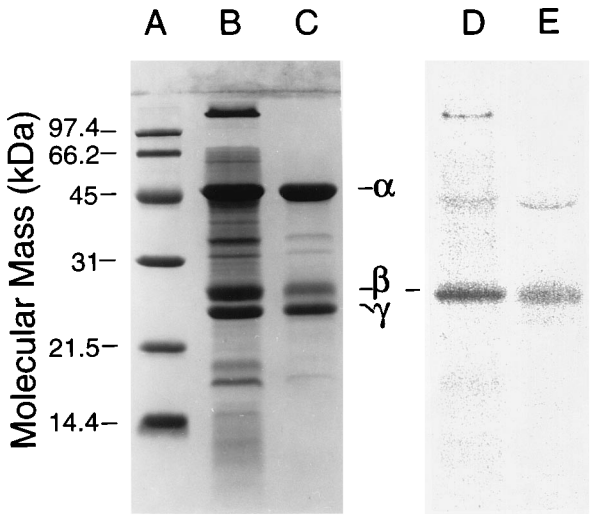

FIG. 3. SDS-polyacrylamide gel electrophoresis of the cell-free fraction isolated from *M. capsulatus* Bath whole cells treated with [U-^{14}C]acetylene using formate as a reductant (lanes B and D) and of purified pMMO treated with [U-^{14}C]acetylene using duroquinol as a reductant (lanes C and E). Lanes A through C were stained for total protein with Coomassie brilliant blue R-250, and lanes D and E are a phosphorescence image of [U-^{14}C]acetylene-labeled polypeptides exposed for 3.5 days on a storage phosphorescence imaging screen. Bio-Rad low-range molecular mass standards are shown in lane A.

(Fig. 2, trace C). The spectrum illustrates the fact that the majority of the iron is EPR silent (2, 3, 24–26). Comparison of the integrated $S = 3/2$ signals for Fig. 2, traces A and B, shows an increase of approximately 26-fold in the level of ferrous iron in the membrane fraction from cells expressing the pMMO. We have identified this ferrous iron atom as the iron center associated with the pMMO (see Fig. 6 and 8).

Purification of the pMMO. Table 2 summarizes the isolation of pMMO from *M. capsulatus* Bath. Several features of the purification procedure described above must be stringently followed to avoid enzyme inactivation. First, supplementation of the growth media with copper and iron increased the specific activity in the detergent-solubilized fraction by fourfold over that in membrane preparations grown in NMS media containing 5 μM $CuSO_4$. Second, the loss of methane oxidation activity was minimized by maintaining anaerobic conditions during solubilization. When in the membrane fraction, the pMMO did not appear to be oxygen sensitive. However, attempts to purify the pMMO under aerobic conditions were not successful. Third, once solubilized, the enzyme was stabilized by maintaining protein concentrations above 15 mg/ml, with maximum activities at 85 mg/ml.

TABLE 2. Purification of pMMO from *M. capsulatus* Bath using 35 mM duroquinol as the in vitro pMMO reductant

Fraction	Amt of protein (mg)	Total activity (nmol · min^{-1} · mg of protein^{-1})	Sp act (nmol · min^{-1} · mg of protein^{-1})	Yield (%)
Whole cell[a]	4,520		60.50	
Cell free	4,382	36,896	8.42	100
Membrane	2,705	28,132	10.40	76
1 M KCl salt-washed membrane	2,312	21,663	9.37	59
Dodecyl β-D-maltoside extract	1,920	18,931	9.86	51
DEAE-cellulose	1,296	13,297	10.26	36
Phenyl-Sepharose CL4B	983	10,892	11.08	30

[a] Formate (20 mM) was used as the pMMO reductant.

pMMO subunit structure. On SDS-polyacrylamide gels the membrane-associated methane oxidation complex consisted of polypeptides with molecular masses of 47,000, 27,000, and 25,000 Da, as well as trace contaminating polypeptides with molecular masses of 37,000, 32,000, and 20,000 Da (Fig. 3, lane C). The 37,000- and 20,000-Da polypeptides were identified as cytochrome *b*-559/569 and copurified with the pMMO. All attempts to remove these polypeptides resulted in enzyme inactivation.

Identification of pMMO polypeptides. Two of the three polypeptides (those with molecular masses of 47,000 and 27,000 Da) were similar to the polypeptides induced when cells expressing the sMMO convert to expression of pMMO under altered growth conditions (13, 15, 43). The identity of the pMMO polypeptides as copper inducible was confirmed by Western blots (immunoblots), labeling with [^{14}C]acetylene, and sequence comparison with *pmo* structural genes.

Acetylene has been shown to be an irreversible inhibitor of both MMOs (44). When different methanotrophs expressing the pMMO were exposed to [^{14}C]acetylene, a major labeled polypeptide was located in the membrane and, with one exception, had a molecular mass of 25,500 to 26,000 Da (15, 44). Figure 3 shows the phosphoimage of the washed membrane fraction (lane D) and purified pMMO (lane E) treated with [^{14}C]acetylene. The increased sensitivity of the phosphorescence image over fluorograms showed the labeling of the 47,000-Da polypeptide as well as the 27,000-Da polypeptide. The labeling of the 47,000-Da polypeptide was reproducible, although the level of labeling was always lower than that observed for the 27,000-Da polypeptide. The labeling of the 47,000-Da polypeptide may result from an activated acetylene intermediate such as ketene which diffuses from the active site and forms a covalent attachment to amino acid residues in the active site or with neighboring polypeptides (44). A similar

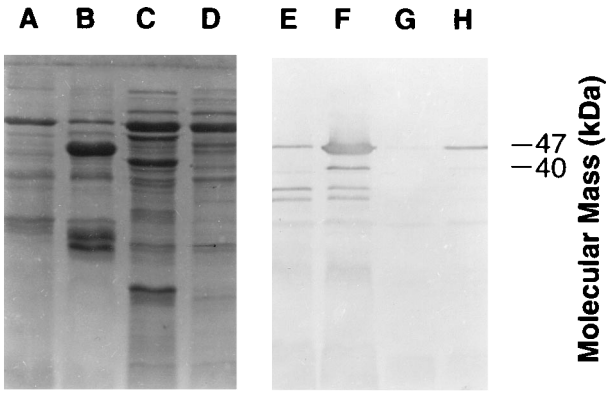

FIG. 4. Immunoblot analysis of *M. capsulatus* (Bath) cell fractions exhibiting soluble or particulate MMO activity with antibodies against pMMO. Results for KCl-washed membrane fractions from cells expressing the sMMO (lanes A [12 μg of protein] and E [36 μg of protein]) and the pMMO (lanes B [12 μg of protein] and F [36 μg of protein]) and for soluble fractions from cells expressing the sMMO (lanes C [16 μg of protein] and G [48 μg of protein]) and the pMMO (lanes D [16 μg of protein] and H [48 μg of protein]) are shown. Lanes A through D were stained with Coomassie brilliant blue R-250. Lanes E through H were probed with antibodies to pMMO.

phenomenon has been observed with the ammonia monooxygenase (28).

Immunoblot analysis of *M. capsulatus* (Bath) cell extracts grown to express either the sMMO or the pMMO with antibodies against the pMMO has confirmed that the 47,000-Da polypeptide was induced by copper in the culture medium (Fig. 4, lane F). Unless the samples were heat treated (100°C for 30 s), a 40,000-Da polypeptide was observed on these immunoblots (Fig. 4F). A 618-Da cofactor has been isolated from the membrane fraction (see below) and shown to be a copper-binding molecule with the ability to form self-aggregating 40,000- and 34,000-Da complexes (59a). The cbc was detected in the extracellular fraction, and not in the membrane fraction, from cells expressing the sMMO.

The identity of the 27,000-Da polypeptide as a copper-inducible polypeptide could not be determined by immunoblot analysis. Staining of the gel with Coomassie brilliant blue R-250 following electrotransfer indicated that only a small percentage of the 27,000-Da polypeptide was transferred to the membrane by using Tris-glycine transfer buffers. Increasing electrotransfer time, removing methanol from the electrotransfer buffers, or altering the pH or ionic strength of the electrotransfer buffers had no effect on the transfer efficiency of the 27,000-Da polypeptide.

The identity of the pMMO polypeptides as switchover polypeptides was also shown by sequence comparisons with the putative pMMO structural genes. Figure 5 shows the N-terminal amino acid sequences of the 47,000-, 27,000-, and 25,000-Da polypeptides, which were similar to the translated amino acid sequences of *M. capsulatus* Bath *pmoA*, *pmoB*, and *pmoC*, respectively (12, 51).

Metal composition. The active enzyme complex contained 2.5 iron and 14.5 copper atoms on the basis of the molecular mass as determined by SDS-polyacrylamide gel electrophoresis, assuming a 1:1:1 subunit ratio and a molecular mass of 99,000 Da. The enzyme preparation contained less than 11 mol% Mo, Mn, and Zn.

Spectral properties. Under low microwave powers, the EPR spectra of the pMMO were similar to those of the washed membrane fraction from cells expressing the pMMO (40, 52) with a type 2 copper center ($g_\perp = 2.057$, $g_\parallel = 2.24$, and $|A|_\parallel = 172$ G) and a weak high-spin iron signal (Fig. 6, trace A). Under higher microwave powers, there was a proportional increase in the intensities of a high-spin ferric signal ($g = 6.0$) and a broad low-field ($g = 12.5$) signal (Fig. 6, traces B and C). This low-field signal has been observed in several mononuclear and binuclear oxygen-binding metal centers, such as those found in cytochrome *c* oxidases, μ-oxo-bridged enzymes, and oxygen-transporting proteins (2, 3, 21, 24–26, 31, 40). In the sMMO, the $g = 15$ signal is observed only with the fully reduced Fe(II)-Fe(II) hydroxylase component (26, 31). In the pMMO from *M. capsulatus* Bath, this signal was observed in the resting sample, suggesting that it does not originate from a μ-oxo-bridged iron center. Reduction of the pMMO with ascorbate and PMS resulted in the loss of the $g = 12.7$ signal in all preparations. The presence of an integer spin signal in pMMO has not been confirmed by parallel-mode EPR experiments.

In contrast to the results of previous studies of membrane samples (40, 52), the "broad isotropic" signal believed to be associated with a novel trinuclear copper cluster and observed under high microwave powers was not detected in the isolated enzyme.

Treatment of reduced pMMO with nitric oxide produced a ferrous-nitric oxide derivative with an electronic spin of $S = 3/2$ (Fig. 6, trace D). The ferrous-nitric oxide derivative EPR spectrum for the pMMO was similar to those for other mononuclear nonheme proteins with *g* values near 4 and 2 (2, 3, 39).

Enzyme activity. Identification by Shiemke et al. (53) of a reductant that directly reduces the pMMO made the isolation of the enzyme possible. When duroquinol was used as a reductant, the purified enzyme oxidized propylene to propylene oxide at rates of 7.8 ± 4.2 nmol · min^{-1} · mg of $protein^{-1}$ at 42°C (the temperature optimum of the enzyme). The rate of propylene oxidation in these samples may have been much higher, since duroquinol became insoluble before saturation levels (above 35 mM) were reached. The pMMO showed a pH optimum of 7.5 with duroquinol as the reductant (Fig. 7).

In preparations of pMMO isolated from cells containing suboptimal concentrations of iron, propylene oxidation activity was stimulated by the addition of ferric iron (Table 3). The stimulation of propylene oxidation by iron was not observed in preparations of pMMO isolated from cells grown in media containing final concentrations of 60 μM Cu and 60 μM iron. Propylene oxidation activity of the enzyme isolated from cells cultured in high-copper and -iron media was more stable and did not require the addition of iron or copper to the reaction mixture for optimal expression.

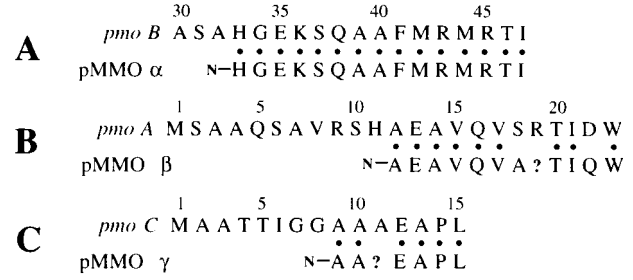

FIG. 5. Sequence alignments showing sequence homology of the individual subunits of the pMMO translated amino acid sequence from the pMMO gene sequence. (A) Sequence alignment of the 47,000-Da (α) polypeptide; (B) sequence alignment of the 27,000-Da acetylene-binding (β) polypeptide; (C) sequence alignment of the 25,000-Da (γ) polypeptide. Dots indicate identical amino acid matches; N indicates the N terminus of the polypeptide. Question marks indicate unidentified amino acids.

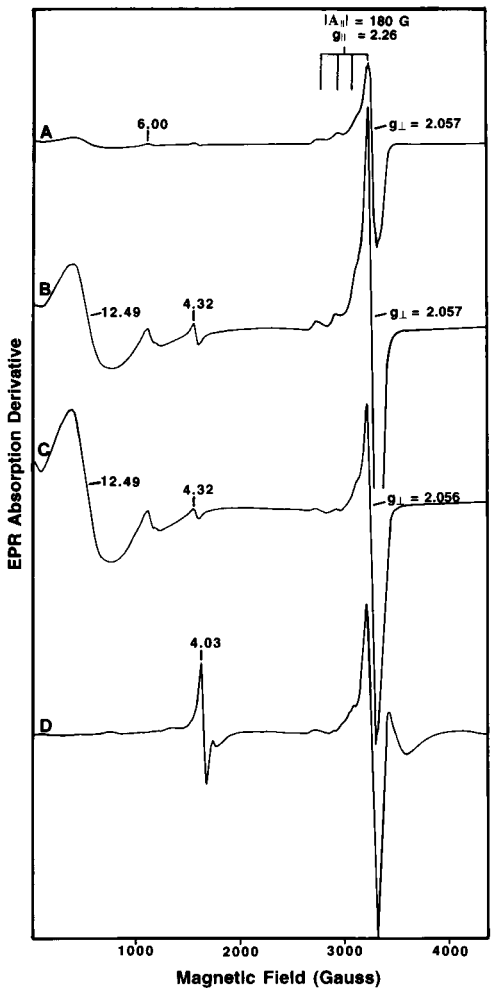

FIG. 6. EPR spectra for pMMO from *M. capsulatus* (Bath) at microwave powers of 0.2 mW (A), 2 mW (B), and 20 mW (C) and that for the nitric oxide derivative of the fully reduced enzyme at a microwave power of 2 mW (D). The protein concentration was 37 mg/ml in 10 mM PIPES (pH 7.0)–0.3% dodecyl maltoside at 8 K. The specific activity for the preparation was 4.8 nmol of propylene oxide · min^{-1} · mg of $protein^{-1}$. Operating parameters were as follows: modulation frequency, 100 kHz; modulation amplitude, 10 G; and time constant, 100 ms. The microwave frequency was 9.429 GHz.

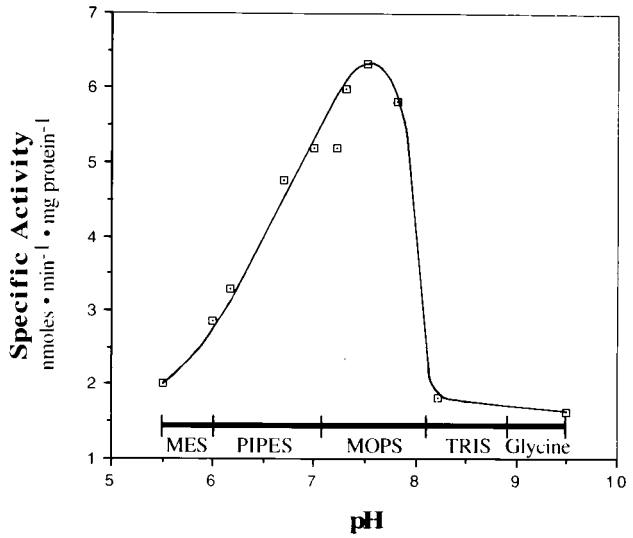

FIG. 7. Effect of pH on propylene oxidation by the isolated membrane-associated MMO from *M. capsulatus* Bath. Reaction mixtures consisted of 600 μl of pMMO extract (39.8 mg of protein) and 35 mM duroquinol in a 7-ml serum vial. Buffer (50-μL additions) was added to a final concentration of 50 mM to samples purified in a buffer containing 10 mM PIPES, pH 7.0 (specific activity = 5.9 nmol · min^{-1} · mg of $protein^{-1}$). MES, 2-(*N*-morpholino)ethanesulfonic acid.

When an enzyme preparation with a propylene oxidation rate of 6.2 nmol · min^{-1} · mg of $protein^{-1}$ was used, the rates of methane and trichloroethylene oxidation were 4.8 nmol · min^{-1} · mg of $protein^{-1}$ and 1.3 nmol · min^{-1} · mg of $protein^{-1}$, respectively. In contrast to the sMMO (9), the isolated enzyme did not oxidize naphthalene.

The activity of the purified enzyme from *M. capsulatus* Bath was destroyed by a single freeze-thaw treatment; heat (100°C for 1 min); proteases; and treatment with acetylene, carbon monoxide, cyanide, and azide (Table 4). Propylene oxidation activity of the purified enzyme was stimulated 1.4-fold by HOQNO and 1.5-fold by myxothiazol (Table 4).

Nature of the pMMO prosthetic groups and isolation of the 47,000- to 27,000-Da switchover polypeptides. Solubilization of pMMO polypeptides in Triton X-100 or CHAPS followed by separation on a sucrose gradient resulted in the loss of enzyme activity. However, this treatment also allowed for the selective isolation of the 47,000- to 27,000-Da pMMO polypeptides. These polypeptides are referred to as the 47,000- to 27,000-Da switchover polypeptides, since they are induced when cells expressing the sMMO convert to expression of the pMMO under different culture conditions (54). The isolation of the switchover polypeptides has provided increased insight into the nature of the prosthetic groups associated with the pMMO (Table 5). The treatment removed the loosely associated copper (i.e., copper associated with the 618-Da cbc) and cytochrome *b*-559/569. Because propylene oxidation activity was absent in Triton X-100 and CHAPS, the identities of these polypeptides as pMMO components were confirmed by N-terminal sequence analysis and purification of $^{14}C_2H_2$-labeled polypeptides from active membrane fractions.

The 47,000- to 27,000-Da switchover fraction contained approximately one nonheme iron atom, one copper atom, and

TABLE 3. Effect of added metal ions on propylene oxidation by the purified pMMO from *M. capsulatus* Bath

Effector	Concn (mM)	Sp act (nmol · min^{-1} · mg of $protein^{-1}$)	Relative activity (% of control)
Control		4.44	100
Cu(I)Cl	1.0	3.00	68
	5.0	2.78	63
$Cu(II)Cl_2$	0.3	5.52	124
	1.0	4.88	110
	5.0	1.08	24
$Fe(II)SO_4$	1.0	3.54	80
	5.0	2.82	64
$Fe(II)SO_4$ + Cys	2.0	<0.60	14
$Fe(III)Cl_3$	0.3	6.72	151
	1.0	7.74	174
	5.0	6.20	140
	10.0	<0.60	14

TABLE 4. Effect of inhibitors on propylene oxidation by whole cells and by the purified pMMO from *M. capsulatus* Bath[a]

Inhibitor	Concn (μM)	% Inhibition or stimulation of propylene oxidation[b]	
		Whole cells	pMMO
KCN	10	96	ND[c]
	50	19	71
	100	0	59
	250	0	27
	500	0	19
	750	0	0
NaN_3	10	69	ND
	50	0	44
	250	0	8
	500	0	0
HOQNO[d]	20	178	136
	50	0	0
Myxothiazol[e]	4	ND	78
	33	ND	85
	164	ND	152
	328	ND	138

[a] Reaction mixtures consisted of purified pMMO (3.0 mg/ml) and 35 mM duroquinol or of whole cells (1 mg/ml) and 20 mM formate as the reductant.
[b] The 100% propylene oxidation rate for whole cells was 78 nmol · min^{-1} · mg of $protein^{-1}$; that for pMMO was 6.2 nmol · min^{-1} · mg of $protein^{-1}$.
[c] ND, not determined.
[d] Solubilized in dimethyl sulfoxide.
[e] Solvent (methanol) removed by evaporation under vacuum.

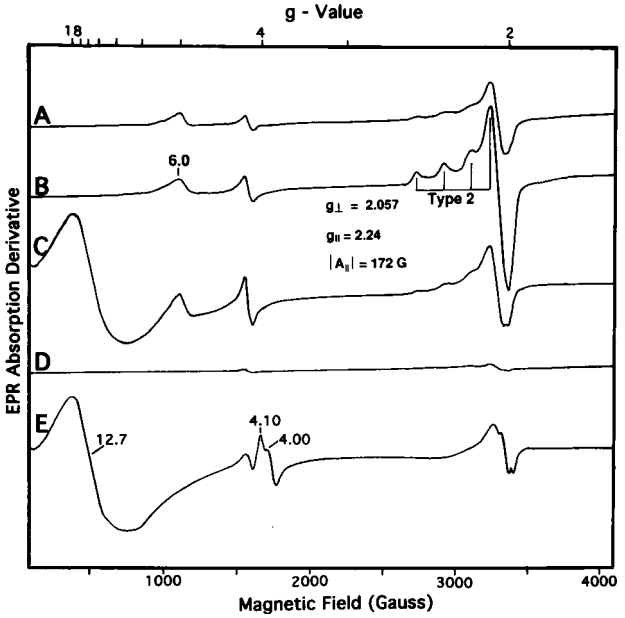

FIG. 8. EPR spectra for the 47,000- to 27,000-Da switchover polypeptides from *M. capsulatus* (Bath). (Trace A) The 47,000- to 27,000-Da switchover polypeptides in 10 mM Tris-HCl–0.1% CHAPS (pH 8.0) (protein concentration, 31 mg/ml); (trace B) 47,000- to 27,000-Da switchover polypeptides in 10 mM Tris-HCl–0.1% Triton X-100 (pH 8.0) (protein concentration, 48 mg/ml); (trace C) acetylene derivative of the 47,000- to 27,000-Da switchover polypeptides purified from $^{14}C_2H_2$-labeled membranes in 10 mM Tris-HCl–0.1% CHAPS (pH 8.0) (protein concentration 34 mg/ml); (trace D) the fully ascorbate-reduced enzyme (protein concentration, 31 mg/ml); (trace E) the nitric oxide derivative of the fully reduced enzyme in 10 mM Tris-HCl–0.1% CHAPS (pH 8.0) (protein concentration, 31 mg/ml). Operating parameters were as follows: modulation frequency, 100 kHz; modulation amplitude, 20 G; microwave power, 2.02 mW; time constant, 100 ms. The microwave frequency was 9.421 GHz.

one acid-labile sulfur atom on the basis of a molecular mass of 74,000 Da. The 47,000- to 27,000-Da switchover complex showed no optical spectra. EPR spectra contained a weak high-spin signal ($g = 6.0$) and the type 2 copper signal observed in the membrane fraction (Fig. 8). The intensity of the type 2 copper signal was highly dependent on the preparation and on the detergent utilized for solubilization of the complex (Fig. 8). In preparations lacking the broad $g = 12.7$ signal, the signal could be generated by the addition of duroquinol and acetylene to the resting sample. As with active pMMO preparations, treatment of the reduced 47,000- to 27,000-Da switchover polypeptides with nitric oxide produced a ferrous-nitric oxide derivative with an electronic spin of $S = 3/2$ (Fig. 8, trace E). Two different techniques have commonly been employed to produce the iron-NO complex for cytochrome *c* oxidase. The first technique is the addition of nitric oxide gas to the reduced enzyme (2, 38). The second technique is the formation of the nitrosyl derivative by the in situ reduction of the nitrite ion (38, 39). Figure 8, trace E, shows the spectrum of the ^{15}N-nitrosyl derivative for the 47,000- to 27,000-Da switchover polypeptides, which was similar to spectra shown by Fig. 2, trace C, and

TABLE 5. Properties of pMMO from *M. capsulatus* Bath

Property	Value(s) for:	
	pMMO	47,000- to 26,000-Da switchover complex
Sp act	7.8 ± 4.2 nmol of propylene · min^{-1} · mg^{-1}	0
Subunit molecular masses (Da)	47,000, 27,000, 25,000	47,000, 27,000
Metal concn (nmol/nmol of enzyme)		
Fe[a]	2.5 ± 0.7[b]	0.9 ± 0.3[c]
Cu[a]	14.6 ± 1.9[b]	0.6 ± 0.1[c]
Cu/Fe	5.8	0.7
EPR signals		
Resting	12.5, 6.0, 4.3, $\|A\|_\parallel$ = 180 G, $g_\parallel$ = 2.26, $g_\perp$ = 2.057	12.7,[d] 6.0, 4.3, $\|A\|_\parallel$ = 172 G, $g_\parallel$ = 2.24, $g_\perp$ = 2.057
Nitric oxide derivative	4.03	4.10, 4.00, 3.95

[a] Values are means ± standard deviations.
[b] Molar enzyme calculations were based on the molecular weight of 99,000 Da determined on SDS-denaturing gels and assumed a 1:1:1 subunit ratio. Protein concentrations were determined by the method of Lowry (33).
[c] The holoenzyme molecular mass was estimated to be 74,000 Da on the basis of a 1:1 stoichiometry of pMMO subunits.
[d] Observation was preparation dependent.

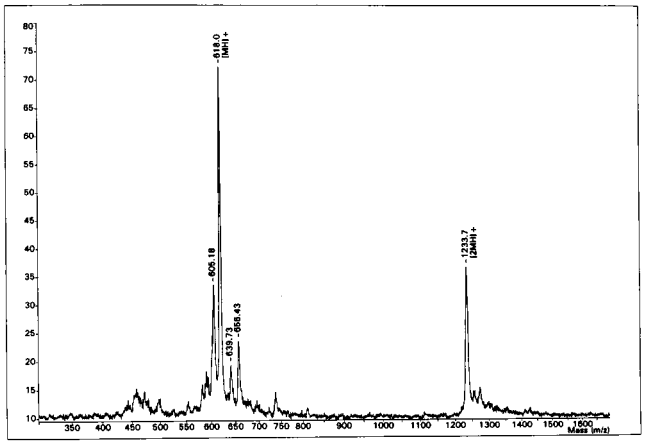

FIG. 9. Matrix-assisted laser desorption ionization mass spectrum of cbc from *M. capsulatus* Bath.

Fig. 6, trace D. Although the spectrum of the $S = 3/2$ species of the 47,000- to 27,000-Da switchover polypeptides showed a striking resemblance to the EPR spectrum for the nitrosyl derivative of protocatechuate 4,5-dioxygenase from *Pseudomonas testosteroni* (32), the $S = 2$ feature at $g = 12.7$ has previously not been observed for dioxygenase enzymes. The lack of nuclear hyperfine structure associated with the $S = 3/2$ center was confirmed by comparison of the ^{15}N-nitrosyl derivative spectra with EPR spectra generated for the ^{14}N-nitrosyl derivative. No detectable changes were observed for subtracted EPR spectra of the ^{14}N-minus ^{15}N-nitrosyl derivatives.

Properties of cbc. The cbc is a small molecule (M_r = 1,200) composed of two identical subunits (618 Da) (Fig. 9). Quantification of the amount of copper per subunit by inductively coupled plasma atomic emission spectroscopy showed that each subunit binds two to three copper atoms. The EPR of the purified sample was complex, having both type 1 ($g_\perp = 2.02$, $g_\parallel = 2.415$, and $|A_\parallel| = 83$ [G]) and type 2 ($g_\perp = 2.035$, $g_\parallel = 2.373$, and $|A_\parallel| = 123$ [G]) copper signals (Fig. 10). EPR spectra from subsaturating levels of copper were shown to emphasize the copper signals. Although we use the terms type 1 and type 2 to describe the two copper centers in the cbc, neither falls directly into this classification (8, 36). The type 1 center showed EPR spectral properties similar to those of other type 1 copper centers, but the absorption spectra were quite different from those of classical type I copper-containing enzymes (Fig. 10 and 11). The type 1 center showed absorption maxima at 245 and 340 nm and no A_{600} (Fig. 11). The absorption spectrum of the cbc was similar to those of metallothioneins (47, 48). The EPR splitting constant of the type 2 center fell between those for type 1 and type 2 centers (36, 47).

Copper titration experiments indicated that the type 1 site is loaded preferentially over the type 2 site (Fig. 10). Figure 11 shows the relationship of changes in A_{245} to copper addition. Optical saturation of the type 1 copper-binding site was achieved at equimolar concentrations of copper.

The addition of *p*-hydroxymercuribenzoate (47) caused the release of copper from the cbc and revealed that less than 30% of the copper was EPR detectable (results not shown). In the study by Nguyen et al. (40) only 30 to 35% of the membrane-associated copper in *M. capsulatus* Bath was detectable by EPR. This difference may reflect the percentage of the cbc that was diamagnetic.

The cellular location of the cbc varied, depending on the copper concentration in the growth medium. In cells cultured

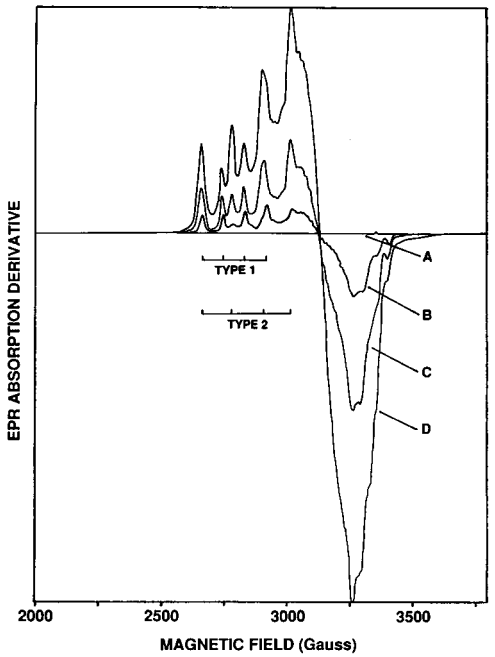

FIG. 10. EPR spectra for the cbc (42.4 mmol) containing 0 mmol of copper (trace A), 1.75 mmol of copper (trace B), 4.24 mmol of copper (trace C), and 5.0 mmol of copper (trace D). Operating parameters were as follows: modulation frequency, 100 kHz; modulation amplitude, 0.25 G; and time constant, 100 ms. The microwave frequency was 9.42 GHz, the gain was 3.3, and the microwave power was 20 dB.

in copper-free medium, the cbc was predominately observed in the extracellular fraction. The cbc isolated from the spent media did not contain copper. The concentration of the cbc in the spent media varied between 0 and 55 mg/liter depending on the copper concentration in the culture media. The decreased concentration of cbc in the spent culture media was associated with an increased concentration of cbc associated with the membrane fraction. Unlike the cbc isolated from the spent media, cbc isolated from the membrane fraction contained two to three copper atoms per mole of cbc. In cells cultured in media containing 5 μM Cu^{2+}, more than 75% of the membrane-associated copper was associated with the cbc.

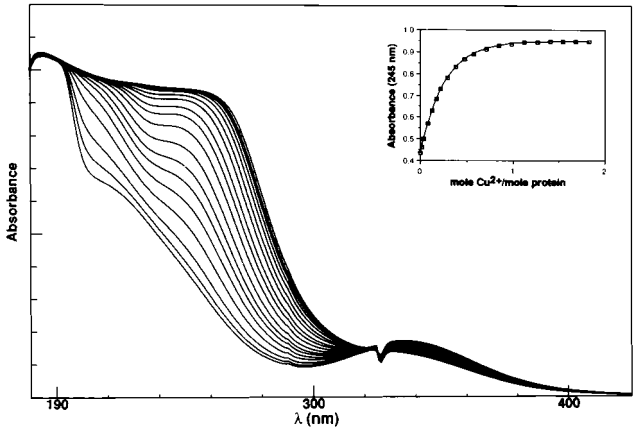

FIG. 11. Absorption spectra of 54 mM copper-free cbc from *M. capsulatus* Bath titrated with $CuCl_2$. The inset shows the relationship of the change in A_{245} to copper addition. For absorbance, the full scale equals 1.2.

DISCUSSION

In contrast to the case with the sMMO, little is known concerning the bioenergetics of methane oxidation by the pMMO. This report describes the initial isolation and characterization of the pMMO as well as some of the biochemical changes related to the expression of the pMMO in *M. capsulatus* (Bath). Nguyen et al. (40) reported that the induction of the pMMO in *M. capsulatus* (Bath) was accompanied by an increase in the concentrations of membrane-associated copper and iron. Although copper resonances were detected and presumed to be associated with the pMMO, no EPR signals to support the observed increase in iron were detected. The results reported in this article show that the majority of the iron associated with the membrane fraction is EPR silent. The EPR spectra of the membrane fraction show a slight increase in the intensity of a high-spin ($g = 6$) signal in the membrane fraction of cells expressing the membrane-associated MMO. However, the majority of the copper-inducible iron in the membrane fraction was EPR detectable only after the formation of a ferrous iron-nitric oxide derivative. The EPR experiments involving the Fe^{2+}-NO derivative in conjunction with elemental analysis of the purified pMMO indicated that the nonheme iron in the pMMO is either a single ferrous iron center, an iron-iron center, or an iron-copper center (2, 3, 24–26). Nitric oxide has been shown to bind to the Fe^{2+}-containing enzymes to yield an EPR spectrum with a characteristic $S = 3/2$ spin system due to the formation of a ferrous-nitrosyl complex (3, 45, 49). The 47,000- to 27,000-Da switchover complex contains a nitric oxide-binding ferrous iron center and was the only membrane-associated NO-binding ferrous iron center present at a high concentration in the membrane fraction from *M. capsulatus* Bath. The observation of copper-induced iron uptake into the membrane fraction lends additional support for the presence of iron in the pMMO.

The pMMO consists of three polypeptides with molecular masses of 47,000, 27,000, and 25,000 Da. The active enzyme contains 2.5 iron atoms and 14.6 copper atoms per 99,000 Da. The majority of the copper associated with the enzyme appears to be associated with a small (618 Da) cofactor that can be separated from the pMMO polypeptides by detergent replacement with CHAPS followed by separation on a sucrose gradient. Once separated, the 47,000- to 27,000-Da switchover polypeptides contain approximately one nonheme iron atom, one copper atom, and one acid-labile sulfur atom. Using the N-terminal amino acid sequence of the 47,000-Da polypeptide purified on SDS-denaturing gels, as well as the ammonia monooxygenase structural genes (6), Semrau et al. (51) and Costello et al. (12) have recently isolated the structural genes for the pMMO. The results reported in this paper verify the identities of *pmoA*, *pmoB*, and *pmoC* as structural genes for the pMMO.

Although it was not apparent on SDS-denaturing gels stained with Coomassie brilliant blue, active preparations of the pMMO contained nonstoichiometric concentrations of cytochrome *b*-559/569. The ratio was estimated from the concentration of protoheme to be approximately 3 to 7 mol% cytochrome *b*-559/569, depending on the preparation. The role, if any, for cytochrome *b*-559/569 in methane oxidation has not been determined. Duroquinol reduction of cytochrome *b*-559/569, as well as methane-dependent reoxidation of ferrous cytochrome *b*-559/569 by pMMO, provides some evidence for a role for this cytochrome as the initial electron donor to the pMMO. However, the majority of the available evidence indicates that cytochrome *b*-559/569 is not directly involved in methane catalysis. First, the concentration of cytochrome *b*-559/569 was unaffected by the expression of pMMO. Second, traditional inhibitors of *b*-type cytochromes (56), HOQNO and myxothiazol, stimulated propylene oxidation at molar ratios commonly observed to completely inhibit *b*-type cytochromes. Third, there was no relation between the level of contaminating cytochrome *b*-559/569 and rates of propylene oxidation in the purified samples. Lastly, the kinetic parameters for quinol oxidation suggested that cytochrome *b* was not the electron acceptor of duroquinol. Duroquinol rapidly reduced cytochrome *b*-559/569 at equimolar concentrations. However, rates of propylene oxidation by isolated enzyme increased proportionally with the duroquinol concentration up to 35 mM, above which duroquinol precipitated out of solution. This observation suggests that a direct electron transfer from duroquinol to pMMO occurred and that the K_m for this reaction is above 35 mM.

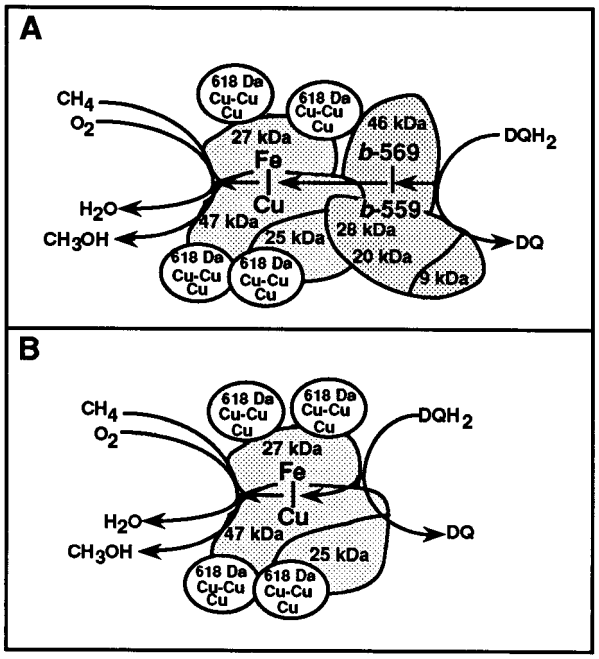

FIG. 12. Proposed mechanisms of methane oxidation by the pMMO using duroquinol (DQ) as a reductant. Models of methane oxidation with cytochrome *b*-559/569 as the initial electron donor (A) and with duroquinol oxidized directly by the pMMO (B) are shown.

The results presented in this paper have led to the development of a working model for the pMMO (Fig. 12). All available evidence indicates that the catalytic site involves both iron and copper, although we have not excluded the possibility of a single ferrous iron center or an iron-iron center. The majority of the copper associated with the pMMO appears to be loosely associated with the enzyme and may provide a secondary function, such as stabilizing the enzyme, maintaining a particular redox state, or sequestering copper. This model is based on the following observations. First, the stoichiometry of copper to iron is one to one in the 47,000- to 27,000-Da switchover polypeptides. Second, the addition of acetylene, an irreversible inhibitor of the pMMO, to the 47,000- to 27,000-Da switchover complex results in the generation of a broad low-field integer spin-like ($g = 12.5$) signal. This integer spin signal has been observed for all known μ-oxo-bridged enzymes, as well as for the copper/heme enzyme cytochrome *c* oxidase (24, 25, 48). Although these two groups of enzymes demonstrate great diversity in structure and function, all enzymes which exhibit this

$S = 2$ signal possess either a mononuclear or a binuclear metal center composed of iron or iron and copper atoms. As with cytochrome oxidase, all enzymes exhibiting an integer spin signal share the ability to bind or interact with oxygen (45).

Nitric oxide derivative EPR spectra of the membrane fractions from cells expressing the pMMO or of purified pMMO also indicate that the enzyme site contains a ferrous iron center. The identity of a ferrous iron center as a switchover copper-induced center was shown by nitric oxide treatment of the membrane fraction from cells expressing the pMMO. The presence of iron in the enzyme was also supported by the observation that Fe^{3+} could serve to activate pMMO activity in purified preparations of *M. capsulatus* Bath pMMO.

The model proposed in this paper differs from the trinuclear copper cluster proposed by Nguyen et al. (40). The trinuclear copper cluster model was based on the correlation of spectral (EPR) changes in the membrane fraction with membrane-associated methane oxidation activity and changes in the elemental (copper and iron) composition of the membrane fraction. The broad isotropic copper signal previously observed by Nguyen et al. (40) was not detected in purified preparations of pMMO. This signal may originate from the cbc, which exhibits a complex EPR spectrum associated with the pMMO. Future studies will address the role, if any, of this cbc, as well as that of cytochrome *b*-559/569, in methane oxidation.

ACKNOWLEDGMENTS

We thank A. B. Hooper, D. M. Arciero, and D. J. Bergman (University of Minnesota) and B. L. Hoyle (ISU) for their evaluation of the manuscript and useful suggestions and F. C. Minion (ISU) for the use of the gel documentation system.

This work was supported by the Iowa State University Office of Biotechnology (ADS) and an Iowa State University Professional Advancement Grant (J.A.Z.).

REFERENCES

1. **Ankent'eva, N. F., and R. I. Govozdev.** 1988. Purification and physiochemical properties of methane monooxygenase from membrane structures of *Methylococcus capsulatus*. Microbiology (New York) **53:**93–96.
2. **Arciero, D. M., and J. D. Lipscomb.** 1986. Binding of ^{17}O-labeled substrate and inhibitors to protocatechuate 4,5-dioxygenase-nitrosyl complex. J. Biol. Chem. **261:**2170–2178.
3. **Arciero, D. M., J. D. Lipscomb, B. H. Huynh, T. A. Kent, and E. Münck.** 1983. Evidence for direct substrate binding to the active site Fe^{2+} of extradiol dioxygenases. J. Biol. Chem. **258:**14981–14991.
4. **Baldwin, M. A., R. Wang, K.-M. Pan, R. Hecker, N. Stahl, B. T. Chait, and S. B. Prusiner.** 1993. Matrix-assisted laser desorption/ionization mass spectrometry of membrane proteins: the scrapie iron protein. Tech. Protein Chem. **9:**41–45.
5. **Beinert, H.** 1983. Semi-micro methods for analysis of labile sulfide and of labile sulfide plus sulfane sulfur in usually stable iron-sulfur proteins. Anal. Biochem. **131:**373–378.
6. **Bergmann, D. D., and A. B. Hooper.** 1994. Sequence of the gene, *amo*B, for the 43-kDa polypeptide of ammonia monooxygenase of *Nitrosomonas europaea*. Biochem. Biophys. Res. Commun. **204:**759–762.
7. **Berry, E. A., and B. L. Trumpower.** 1987. Simultaneous determination of hemes *a*, *b*, and *c* from pyridine hemochrome spectra. Anal. Biochem. **161:** 1–15.
8. **Boas, J. F.** 1984. Electron paramagnetic resonance of copper proteins, p. 5–62. *In* R. Lontei (ed.), Copper proteins and copper enzymes, vol. I. CRC Press, Inc., Boca Raton, Fla.
9. **Brusseau, G. A., H.-C. Tsien, R. S. Hanson, and L. P. Wackett.** 1990. Optimization of trichloroethylene oxidation by methanotrophs and the use of colorimetric assay to detect soluble methane monooxygenase activity. Biodegradation **1:**19–29.
10. **Cardy, D. J. N., V. Laidler, G. P. C. Salmond, and J. C. Murrell.** 1991. Molecular analysis of the membrane monooxygenase (MMO) gene cluster of *Methylosinus trichosporium* OB3b. Mol. Microbiol. **5:**335–342.
11. **Cheesman, M. R., N. L. Watmough, C. A. Pires, R. Tuner, T. Brittain, R. B. Gennis, C. Greenwood, and A. J. Thomson.** 1993. Cytochrome *bo* from *Escherichia coli*: identification of haem ligands and reaction of the reduced enzyme with carbon monoxide. Biochem. J. **289:**709–718.
12. **Costello, A. M., T. L. Peeples, and M. E. Lidstrom.** Personal communications.
13. **Dalton, H., S. D. Prior, D. J. Leak, and S. H. Stanley.** 1984. Regulation and control of methane monooxygenase, p. 75–82. *In* R. L. Crawford and R. S. Hanson (ed.), Microbial growth on C_1 compounds. American Society for Microbiology, Washington, D.C.
14. **DiSpirito, A. A.** 1990. Soluble cytochromes from *Methylomonas* A4. Methods Enzymol. **188:**289–297.
15. **DiSpirito, A. A., J. Gulledge, A. K. Shiemke, J. C. Murrell, M. E. Lidstrom, and C. L. Krema.** 1992. Trichloroethylene oxidation by the membrane-associated methane monooxygenase in type I, type II and type X methanotrophs. Biodegradation **2:**151–164.
16. **DiSpirito, A. A., A. K. Shiemke, S. W. Jordan, J. A. Zahn, and C. L. Krema.** 1994. Cytochrome aa_3 from *Methylococcus capsulatus* Bath. Arch. Microbiol. **161:**258–265.
17. **Ferguson-Miller, S., D. L. Brautigan, and E. Margoliash.** 1976. Correlation of the kinetics of electron transfer activity of various eukaryotic cytochromes *c* with binding to mitochondrial cytochrome *c* oxidase. J. Biol. Chem. **251:** 1104–1115.
18. **Fox, B. G., W. A. Froland, J. E. Dege, and J. D. Lipscomb.** 1989. Methane monooxygenase from *Methylosinus trichosporium* OB3b. J. Biol. Chem. **264:** 10023–10033.
19. **Fox, B. G., K. K. Surerus, E. Münck, and J. D. Lipscomb.** 1988. Evidence for a μ-oxo-bridged binuclear iron cluster in the hydroxylase component of methane monooxygenase. J. Biol. Chem. **263:**10553–10556.
20. **Fuhrhop, J.-H.** 1975. Laboratory methods in porphyrin and metalloporphyrin research. Elsevier Scientific Publishers, New York.
21. **Galpin, J. R., G. A. Veldink, J. F. G. Vliegenthart, and J. Boldingh.** 1978. The interaction of nitric oxide with soybean lipoxygenase-1. Biochim. Biophys. Acta **536:**356–362.
22. **Green, J., and H. Dalton.** 1985. Protein B of soluble methane monooxygenase from *Methylococcus capsulatus* (Bath). A novel regulatory protein of enzyme activity. J. Biol. Chem. **260:**15795–15802.
23. **Green, J., and H. Dalton.** 1989. Substrate specificity of soluble methane monooxygenase: mechanistic implication. J. Biol. Chem. **264:**17698–17703.
24. **Hagen, W. R.** 1982. EPR of non-kramers doublet in biological systems, characterization of an $S = 2$ system in oxidized cytochrome *c* oxidiase. Biochim. Biophys. Acta **708:**82–98.
25. **Hendrich, M. P., E. Münck, B. G. Fox, and J. D. Lipscomb.** 1990. Inter-spin EPR studies of the fully reduced methane monooxygenase hydroxylase component. J. Am. Chem. Soc. **112:**5861–5865.
26. **Hendrich, W. P., and P. G. Debrunner.** 1989. Integer-spin electron paramagnetic resonance of iron proteins. Biophys. J. **56:**489–506.
27. **Hyman, M. R., and D. J. Arp.** 1990. The small-scale production of [U-14C] acetylene from $Ba^{14}CO_3$: application to labeling of ammonia monooxygenase in autotrophic nitrifying bacteria. Anal. Biochem. **190:**348–353.
28. **Hyman, M. R., and D. J. Arp.** 1992. $^{14}C_2H_2$- and $^{14}CO_2$-labeling studies of the *de novo* synthesis of polypeptides by *Nitrosomonas europaea* during recovery from acetylene and light inactivation of ammonia monooxygenase. J. Biol. Chem. **267:**1534–1445.
29. **Laemmli, U. K.** 1970. Cleavage of structural proteins during the assembly of the head of bacteriophage T4. Nature (London) **227:**680–685.
30. **Lidstrom, M. E.** 1988. Isolation and characterization of marine methanotrophs. Antonie van Leeuwenhoek J. Microbiol. Serol. **54:**189–199.
31. **Lipscomb, J. D.** 1994. Biochemistry of the soluble methane monooxygenase. Annu. Rev. Biochem. **48:**371–399.
32. **Lipscomb, J. D., J. W. Whittaker, and D. M. Arciero.** 1982. Comparative studies of intra- and extradiol protocatechuate dioxyphases, p. 27–38. *In* M. Nizaju, S. Yamamoto, Y. Ishimura, M. J. Coon, L. Ernster, and R. W. Estabrook (ed.), Oxygenases and oxygen metabolism. Academic Press, New York.
33. **Lowry, O. H., N. J. Rosebrough, A. L. Farr, and R. J. Randall.** 1951. Protein measurement with the Folin phenol reagent. J. Biol. Chem. **193:**265–275.
34. **Lund, J., and H. Dalton.** 1985. Further characterization of the FAD and Fe_2S_2 redox centers of component C, the NADH:acceptor reductase of the soluble methane monooxygenase of *Methylococcus capsulatus* (Bath). Eur. J. Biochem. **147:**291–296.
35. **Mak, A. S., and B. L. Jones.** 1978. Application of S-pyridylethylation of cysteine to sequence analysis of proteins. Anal. Biochem. **83:**432–440.
36. **Malmström, B. G., B. Reinhammar, and T. Vänngård.** 1970. The state of copper in stellacyanin and laccase from the lacquer tree *Rhus vernicifera*. Biochim. Biophys. Acta **205:**48–57.
37. **McDonnel, A., and L. A. Staehelin.** 1981. Detection of cytochrome *f*, a *c*-class cytochrome, with diaminobenzidine in polyacrylamide gels. Anal. Biochem. **117:**40–44.
38. **Moss, R. H., and S. I. Chan.** 1980. Electron paramagnetic resonance studies of nitrosyl ferrous heme complexes. Determination of an equilibrium between two conformations. J. Biol. Chem. **255:**7876–7882.
39. **Nelson, M. J.** 1987. The nitric oxide complex of ferrous soybean lipoxygenase-1. J. Biol. Chem. **262:**12137–12142.
40. **Nguyen, H.-N., A. K. Shiemke, S. J. Jacobs, B. J. Hales, M. E. Lidstrom, and S. I. Chan.** 1994. The nature of the copper ions in the membranes containing the particulate methane monooxygenase from *Methylococcus capsulatus*

(Bath). J. Biol. Chem. **269:**14995–15005.
41. **Patel, R. N., and J. C. Savas.** 1987. Purification and properties of the hydroxylase component of methane monooxygenase. J. Bacteriol. **169:**2313–2317.
42. **Pilkington, S. J., and H. Dalton.** 1991. Purification and characterization of the soluble methane monooxygenase from *Methylosinus sporium* demonstrates the highly conserved nature of the enzyme in methanotrophs. FEMS Microbiol. Lett. **78:**103–108.
43. **Prior, S. D., and H. Dalton.** 1985. The effect of copper ions on membrane content and methane monooxygenase activity in methanol-grown cells of *Methylococcus capsulatus* (Bath). J. Gen. Microbiol. **131:**155–163.
44. **Prior, S. D., and H. Dalton.** 1985. Acetylene as a suicide substrate and active site probe for membrane monooxygenase from *Methylococcus capsulatus* (Bath). FEMS Microbiol. Lett. **29:**105–109.
45. **Rich, P. R., J. C. Salerno, J. S. Leigh, and W. D. Bonner, Jr.** 1978. A sin 3/2 ferrous-nitric oxide derivative of an iron-containing moiety associated with *Neurospora crassa* and higher plant mitochondria. FEBS Lett. **93:**323–325.
46. **Robinson, J., and J. M. Cooper.** 1970. Method of determining oxygen concentrations in biological media, suitable for calibration of oxygen electrode. Anal. Biochem. **33:**390–399.
47. **Rupp, H., R. Cammack, H.-J. Harmann, and U. Weser.** 1979. Oxidation-reduction reactions of copper-thiolate centers in Cu-thionein. Biochim. Biophys. Acta **578:**462–475.
48. **Rupp, H., and U. Weser.** 1974. Conversion of metallothionein into Cu-thionein, the possible low molecular weight form of neonatal hepatic mitochondrocuprein. FEBS Lett. **44:**293–297.
49. **Salerno, J. C., and J. N. Seidow.** 1979. The nature of the nitric oxide complexes of lipoxygenase. Biochim. Biophys. Acta **579:**246–251.
50. **Scott, D., J. Brannan, and I. J. Higgins.** 1981. The effect of growth conditions on intracytoplasmic membranes and methane monooxygenase activities in *Methylosinus trichosporium* OB3b. J. Gen. Microbiol. **125:**63–72.
51. **Semrau, J. D., A. Chistoserdov, J. Lebron, A. Costello, J. Davagnino, E. Kenna, A. J. Holmes, R. Finch, J. C. Murrell, and M. E. Lidstrom.** 1995. Particulate methane monooxygenase genes in methanotrophs. J. Bacteriol. **177:**3071–3079.
52. **Semrau, J. D., D. Zolandz, M. E. Lidstrom, and S. I. Chan.** 1995. The role of copper in the pMMO *Methylococcus capsulatus* Bath: a structural *vs*. catalytic function. J. Inorg. Chem. **58:**235–244.
53. **Shiemke, A. K., S. A. Cook, T. Mily, and P. Singleton.** 1995. Detergent solubilization of membrane-bound methane monooxygenase requires plastoquinol analogs as electron donors. Arch. Biochem. Biophys. **321:**521–528.
54. **Stanley, S. H., S. D. Prior, D. J. Leak, and H. Dalton.** 1983. Copper stress underlines the fundamental change in intracellular location of methane mono-oxygenase in methane utilizing organisms: studies in batch and continuous cultures. Biotechnol. Lett. **5:**487–492.
55. **Tonge, G. M., D. E. F. Harrison, and I. J. Higgins.** 1977. Purification and properties of the methane mono-oxygenase from *Methylosinus trichosporium* OB3b. Biochem. J. **161:**333–334.
56. **von Jagow, G., and T. A. Link.** 1986. Use of specific inhibitors on the mitochondrial bc_1 complex. Methods Enzymol. **126:**253–271.
57. **Whittenbury, R., and H. Dalton.** 1981. The methylotrophic bacteria, p. 894–902. *In* M. P. Starr, H. G. Truper, A. Balows, and H. G. Schlegel (ed.), The prokaryotes, vol. I. Springer-Verlag, New York.
58. **Williams, J. N.** 1964. A method for the simultaneous quantitative estimation of cytochrome *a*, *b*, *c*, and *f* in mitochondria. Arch. Biochem. Biophys. **107:**537–543.
59. **Woodland, M. P., and H. Dalton.** 1984. Purification and characterization of component A of the methane monooxygenase from *Methylococcus capsulatus* (Bath). J. Biol. Chem. **259:**53–60.
59a. **Zahn, J. A., and A. A. DiSpirito.** Unpublished data.
60. **Zahn, J. A., C. Duncan, and A. A. DiSpirito.** 1994. Oxidation of hydroxylamine by cytochrome P-460 of the obligate methylotroph *Methylococcus capsulatus* Bath. J. Bacteriol. **176:**5879–5887.